

ANN-Based SVC for Optimal Performance of Wind-Driven Self-Excited Synchronous Reluctance Generator

Mostafa Rida*[‡], Adel El Samahy*, Essam Rashad**, Mohamed El Korfolly*, Erhab Youssef*

*Department of Electrical Power and Machines, Faculty of Engineering, Helwan University (FEHU), Cairo, Egypt

**Department of Electrical Power and Machines, Faculty of Engineering, Tanta University (FETU), Tanta, Egypt

(Mostafarida@h-eng.helwan.edu.eg, a.elsamahy@h-eng.helwan.edu.eg, Emrashad@ieec.org, mohamed_elkorfolly@h-eng.helwan.edu.eg, erhabyoussef@h-eng.helwan.edu.eg)

[‡]Corresponding Author; Mostafa Rida, Department of Electrical Power and Machines, Faculty of Engineering, Helwan University, Helwan, Cairo, 1 Sherif st., Helwan, 11792, Helwan, Egypt
, Mostafarida@h-eng.helwan.edu.eg

Received: 28.10.2022 Accepted: 23.11.2022

Abstract- Renewable energy (RE) has been embraced as one of the primary solutions to reduce the impacts of the global warming phenomenon linked with temperature rise due to the pollution inherent particularly from fossil fuels and conventional resources. Self-Excited Synchronous Reluctance Generator (SESRG) is one of the cost-effective ways in wind energy conversion systems. The SESRG has distinct characteristics that make it an attractive candidate for wind turbines, such as there is a cageless rotor and free Permanent Magnet, the manufacturing, and maintenance costs are comparatively economical. Additionally, it offers a fault-tolerant machine that can operate at high speeds and temperatures. However, the terminal voltage is affected by any change in either load currents or variable wind speed. Subsequently, the excitation capacitances should be varied to meet the required reactive power. Furthermore, during unbalanced operations, the unbalanced terminal voltage and stator currents of SESRG are generated, introducing positive, negative, and zero sequence components. That produces a ripple torque that causes mechanical stress on the rotor shaft, in addition to the temperature rise of the stator winding. Therefore, this article presents an Artificial Neural Network (ANN) based on a Static VAR Compensator (SVC) to predict the suitable excitation capacitance required to deliver the reactive power for any load condition or wind speed. By predicting the excitation capacitance for each phase individually that is required to mitigate the unbalanced condition. The validation simulation results are performed using the MATLAB/Simulink platform.

Keywords- Synchronous Reluctance Generator; Induction Generator, Permanent Magnet Synchronous Generator, Stand-Alone; Artificial Neural Network; Voltage control Static VAR Compensators; Thyristor-Controlled Reactor.

1. Introduction

Due to energy demand increases and climate changes caused by global warming, renewable becomes essential to moderate such effects. In recent years, renewable energy is getting strong worldwide attention. Examples of such sources are hydropower, geothermal power, solar energy, and wind energy [1]. A Synchronous Reluctance Generator (SRG) has been usefully used in stand-alone Wind Energy Conversion Systems (WECS), because of its brushless and rugged construction, low cost, maintenance and, operational simplicity, self-protection against faults, good dynamic response, and capability to generate power at varying speeds [2], [3]. Furthermore, features such as low core loss, low noise, and no rotor copper loss. Then, at that point, SESRG exhibits characteristics highly attractive for stand-alone WECS applications [3]-[5]. The SESRG is a popular alternative generator in stand-alone WECS, but the build-up voltage process generally requires an external reactive power source connected to the stator terminals like a three-phase excitation capacitance [6], [7]. However, the magnitude of the SESRG terminal’s voltage and frequency are significantly affected by variations in load impedance and the speed of prime-mover [8]-[10].

In addition, the operation under unbalanced load conditions results in unbalanced terminal voltages and stator currents. Consequently, the positive, negative, and zero sequence components are created [11]. The unbalanced stator currents produce a ripple torque that causes mechanical stress on the rotor shaft, in addition to the temperature rise of the stator, which degrades the stator winding insulation [12]-[15]. The quality of accepting the SESRG relies on the ability of the control system to give a constant voltage at different values for load impedance and prime-mover speed and eliminates the unbalanced voltage due to the unbalanced load [7]. The SVC is one of the power electronics solutions that offer significant advantages for voltage control and reactive power control purposes due to its simplicity and lower cost [6], [16]. They generally can be used as a compensator for solving machine problems in balanced and unbalanced load conditions [7], [16].

In this article, The SVC is proposed to control the terminal voltage of SESRG driven by a wind turbine to keep it at desired value regardless of the change in load and wind speed. In addition, it is used to eliminate the unbalance terminal voltage during an unbalanced load. The implementation of SVC used is a Fixed Capacitor and thyristor Controlled reactor (FC-TCR). The terminal voltage is controlled by adaptation in the excitation capacitance using SVC depending on predicted excitation capacitance by ANN.

The main contribution of this article focuses on enhancing the generator operation during balanced and unbalanced operations by implementing an ANN based on a Static VAR Compensator. The proposed control technique is a low-cost, simple, and online prediction with a high response rate. It is dependent on the online prediction of excitation capacitance based on ANN that has been trained using previously collected data. The predicted excitation

capacitance is used for online calculation of The TCR firing angle that is required to provide the effective excitation capacitance. Consequently, the terminal voltage is regulated to be constant at the desired value regardless of any change in load condition or wind speed. In addition to studying the SESRG performance under unbalanced load conditions, which has not been addressed by researchers since January of 2000. In this instance, the controller is attempting to reduce the unbalanced condition in order to reduce the unbalance affection on both the load and the generator. The ANN provides separate excitation capacitance for each phase individually, which aids in minimization of the unbalance condition and its consequences by 50% compared to the fixed capacitance case.

This article is organized as follows: Firstly, the proposed system of stand-alone SESRG driven by a wind turbine, controlled by using the Static Var Compensator based on an artificial neural network is modeled in detail. Secondly, the results of the SESRG during a balanced load condition at various load and wind speed operations are discussed, in addition to the fault mitigation for the SESRG during unbalanced load operations is investigated as well, and finally, the conclusion is presented in the last section.

2. Wind-Driven SESRG System Modelling

In this article, the proposed system is SRG driven by a wind turbine as a stand-alone system and supplies a three-phase static load, as shown in Fig.1. The SVC is FC-TCR type and connected to each phase to regulate the terminal voltage and keep it constant. The ANN control is an online prediction of the required excitation capacitance for each phase (C_a, C_b, C_c) individually and then calculates the firing angle for each TCR to control the reactive power under various conditions.

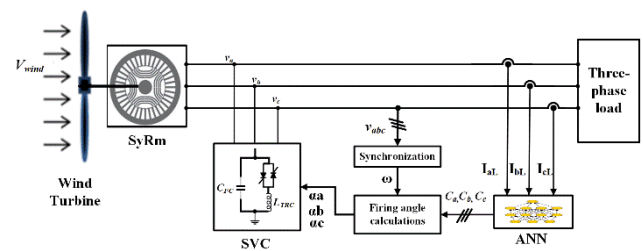


Fig.1. Schematic diagram of the proposed system.

2.1. Wind Turbine

The wind turbine is a well-known technology that extracts the energy stored in the wind and converts it into a mechanical energy form [2], [3], [6]. The wind turbine model is obtained by using the characteristics equations mentioned below.

The extracted mechanical output power of a wind turbine is getting by:

$$P_m = \frac{1}{2} C_p(\lambda, \beta) \rho A V_{wind}^3 \tag{1}$$

where P_m , C_p , λ , β and ρ are the mechanical output power in (watt), rotor power coefficient of the turbine, tip speed

ratio(TSR), and blade pitch angle in (degree), respectively. While A and V_{wind} are the air density in kg/m^3 , turbine swept area in (m^2), and wind speed in (m/s), respectively.

The rotor power coefficient characteristic depends mainly on blade pitch angle and TSR. Consequently, the rotor power coefficient is expressed as a function of (λ, β),

$$C_p(\lambda, \beta) = c_1 e^{\frac{-c_5}{\lambda_i}} \left(\frac{c_2}{\lambda_i} - c_3 * \beta - c_4 \right) + c_6 \lambda \quad (2)$$

$$\frac{1}{\lambda_i} = \left(\frac{1}{\lambda + 0.08\beta} - \frac{0.035}{1 + \beta^3} \right) \quad (3)$$

where c_1-c_6 are constant coefficients, $c_1=0.5176$, $c_2=116$, $c_3=0.4$, $c_4=5$, $c_5=21$ and $c_6=0.0068$. The tip speed ratio TSR is defined as the ratio of the linear speed of the turbine blade to the wind speed.

$$\lambda = \frac{R \omega_t}{V_{wind}} \quad (4)$$

where ω_t and R represent the rotor blade speed in rad/s and the turbine blade radius in meters, respectively.

The mechanical output torque developed by the wind turbine (T_m) is given by:

$$T_m = \frac{P_m}{\omega_t} \quad (5)$$

2.2. SESRG Modelling

The SESRG dynamic model is derived using Park's d-q axes transformation and simplified by using some assumptions that are considered in [2]-[4].

The steady-state model equations of SESRG were obtained by making all flux linkage rates change to zero. Hence, the steady-state model in the d-q rotor reference frame is expressed using Eq. (6) and (7) listed by [17], [18].

$$V_{ds} = -r_s i_d - \frac{\omega_r}{\omega_b} X_q i_q \quad (6)$$

$$V_{qs} = -r_s i_q + \frac{\omega_r}{\omega_b} X_d i_d \quad (7)$$

where (V_{qs}, V_{ds}) are the stator voltage in q-d axes frame, (i_q, i_d) are stator currents in d-q axes, r_s represents stator resistance, (X_d, X_q) are the stator direct and quadrature axis reactance respectively at base frequency, while ω_b and ω_r are the synchronous and rotor speeds in rad/s, respectively.

The flux linkages in d-q axis coordinators can be obtained by:

$$\lambda_q = -L_q i_q \quad (8)$$

$$\lambda_d = -L_d i_d \quad (9)$$

where L_d and L_q are the stator inductors in the direct and quadrature axis respectively.

Hence, the electromagnetic torque developed T_e by the generator is obtained by Eq. (10) and by substituting Eq. (8) and Eq. (9) in Eq. (10). The electromagnetic torque is expressed as a function of inductance in (11) where P is the number of poles of the SRG.

$$T_e = \frac{3}{4} P (\lambda_d i_q - \lambda_q i_d) \quad (10)$$

$$T_e = \frac{3}{4} P (L_d - L_q) i_d i_q \quad (11)$$

Refereeing to [4], [16], the equations of load voltage and currents in d-q axis frame can be determined as described by Eq. (12) and (13), where v_{dL}, v_{qL}, i_{dL} , and i_{qL} are the load voltages and the load currents in d-q axis, respectively.

$$i_{qL} = \frac{1}{L_L} \int (v_{qL} - i_{qL} R_L - w_r L_L i_{dL}) dt \quad (12)$$

$$i_{dL} = \frac{1}{L_L} \int (v_{dL} - i_{dL} R_L + w_r L_L i_{qL}) dt \quad (13)$$

The current of the excitation capacitance in the d-q axis can be obtained by Eq. (14) and (15) [3], [16].

$$i_d - i_{dL} = -w_r C v_{qL} + C \frac{dv_{dL}}{dt} \quad (14)$$

$$i_q - i_{qL} = w_r C v_{dL} + C \frac{dv_{qL}}{dt} \quad (15)$$

where i_d is calculated as a function of X_d , which is obtained at base frequency [18], using Eq. (16). The Curve fitting is used to model a 4th-order polynomial function based on the magnetization curve of a 5.5 kW SRG.

$$i_d = 3.723 * 10^{-8} X_d^4 - 0.001271 X_d^3 + 0.1534 X_d^2 - 6.393 X_d + 97.03 \quad (16)$$

The excitation capacitor value necessary to operate the SESRG at any load conditions or speed profile. Whereas it is calculated initially using the steady-state equations as discussed in [4], [18].

2.3. Static VAR Compensator Modelling

The static VAR compensator (SVC) is used widely as a shunt compensator device for voltage control in power systems and wind turbine generators [7]. Generally, it consists of a fixed-shunt capacitance FC and thyristor-controlled Reactor (TCR), as shown in Fig. 2. The TCR is a variable reactance controlled by the firing angle of bi-directional thyristors connected in series with an inductor to continuous adaptation for the excitation capacitance connected at each phase individually (C_a, C_b, C_c).

The affected capacitance value (C_{eff}) is obtained by The TCR firing angle (α) control. The TCR firing angle varies from 90° (inductive mode) to 180° (capacitive mode) using Eq. (19) [16] and [19].

$$C_{eff} = C_{FC} - \frac{1}{W_b^2 - L_{TCR}} \left(2 - \frac{2\alpha}{\pi} - \frac{\sin 2\alpha}{\pi} \right) \quad (17)$$

where C_{FC} and L_{TCR} are the fixed capacitance and TCR inductance, respectively.

The TCR inductance depends on C_{max} , C_{min} the maximum and minimum excitation capacitance required, respectively, obtained as explained in [6] and [7]. The TCR inductance can be obtained using the following equation.

$$L_{TCR} = \frac{1}{\omega_b^2(C_{max}-C_{min})} \tag{18}$$

The effective capacitance value varies between C_{min} and C_{max} by controlling the firing angle from 90° to 180° .

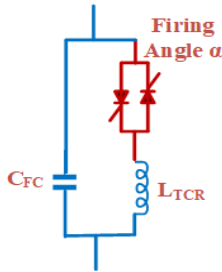


Fig.2. FC-SVC schematic diagram.

3. Artificial Neural Network

Artificial Neural Networks (ANN) offer a different solution for presenting the linear and nonlinear curve fitting issues [20]. The system's dynamic model does not require it can learn to represent any complex function and nonlinear interactions. Neural networks are generally approximators because they can approximate any complex function irrespective of its linearity [20] and [21]. This technique is more practical with signal processing, pattern recognition, function approximation, and classification [22]-[25].

In the case of the SESRG proposed system, the required value of excitation capacitance is predicted for each loading condition and wind speed. Since the regression model between the loading conditions and the predicted capacitance value has been created using the ANN, the regression function (R) can be redefined by using mapping of various operating conditions and expressed using Eq. (19).

$$R = f(I_L, pf, V_{wind}) \tag{19}$$

where I_L , pf , and V_{wind} are the load current, load power factor and wind speed respectively.

The regression function is used to define the predicted excitation capacitance value (C_{NN}) [26]-[28].

In this paper, the regression mapping function is trained using a feed-forward back-propagation ANN with hidden layers. The ANN training process is prepared and validated by a previously collected database of proper inputs and the corresponding target output, where inputs are (I_L , pf , and V_{wind}), while the corresponding target output is C_{NN} , as shown in Fig 3. Consequently, the required firing to adapt the effective excitation capacitance C_{eff} at C_{NN} is obtained using Eq. (17).

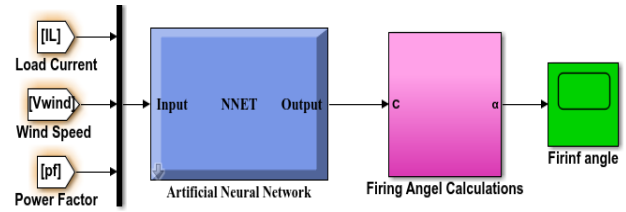


Fig.3. The proposed ANN Model for SERSG

The proposed ANN model performance is estimated by the Mean Squared Error (MSE), where the training is stopped at a very small value. Figure 4 shows the variation of the MSE with the iterations, the MSE for the test set and the validation set are the same characteristics and very small values. As well, there is the regression plot that displays the ANN output concerning the required targets. Figure 5 depicts an excellent fit between the targets and output values for the training process, validation, and the test.

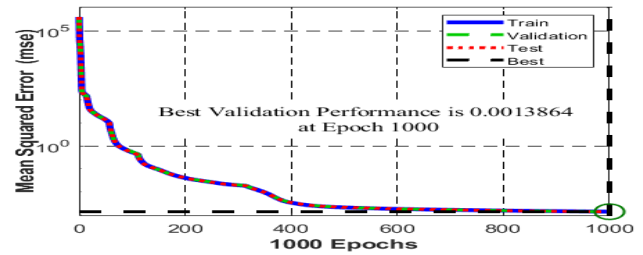


Fig.4. The ANN Mean square Error variation

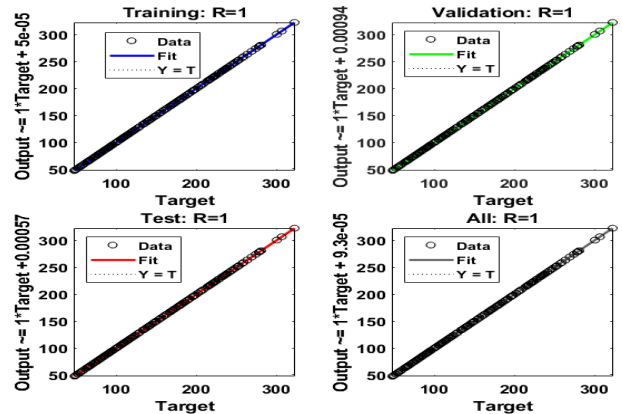


Fig.5. The ANN Regression plot performance

For more validation, Fig.6 shows a perfect agreement between the predicted capacitance value by ANN and the calculated capacitance value by the steady-state machine equations.

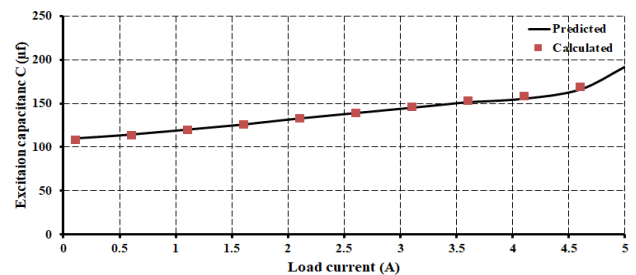


Fig.6. Predicted and calculated excitation capacitance at 50Hz.

4. Results and Discussions

This section presents the generator performance under balanced and unbalanced conditions, in addition to showing the enhancing operation of SERG in either balanced or

unbalanced operations by using the SVC based on the ANN technique. MATLAB/Simulink is employed to model the complete system as shown in Fig.7.

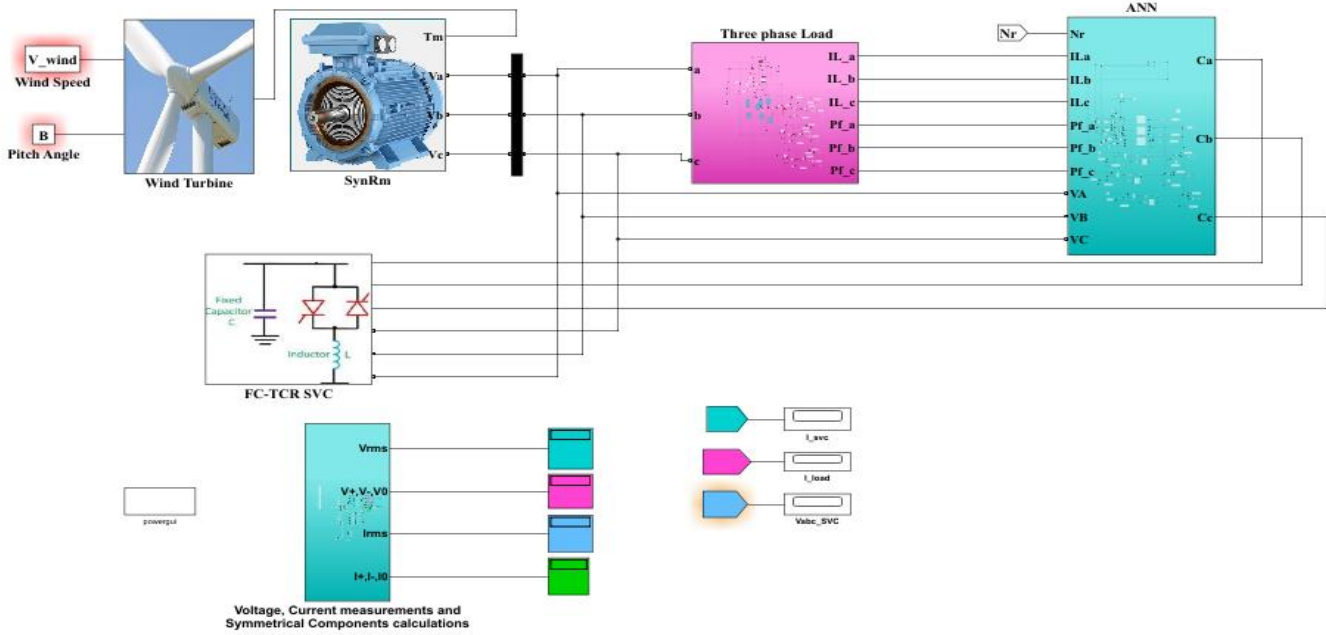


Fig.7. schematic diagram of the proposed system using MATLAB/Simulink.

Firstly, the analytical performance is studied for four poles 5.5 kW, 50Hz, and 350 V SRG. The SRG parameters are predetermined using simple standard off-line tests like DC, locked rotor, and no-load tests presented in [18], [29] and listed in table (1). The SRG magnetizing characteristics are given by the i_d - X_d curve obtained by no load test as shown in Fig.8.

Table 1. Machine parameters at 50Hz

Machine rating (kW)	Terminal voltage (V)	R_s (Ω)	Unsaturated L_d (H)	Unsaturated L_q (H)	Rated speed (r.p.m)
5.5	340	0.6	0.1331	0.05195	1500

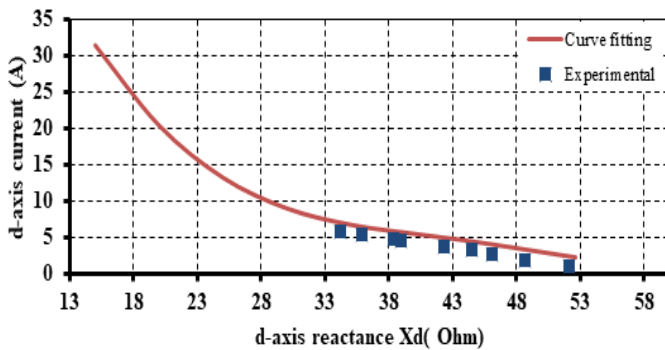


Fig.8. The magnetizing characteristics of the SESRG machine at base frequency.

4.1. Case Study I

4.1.1. Balanced Operation with Constant Excitation Capacitance.

This case presents the results of stand-alone SESRG driven by a wind turbine under both variable speed and variable load, while the excitation capacitance value is kept constant.

Firstly, the wind speed and excitation capacitance are kept constant, whereas the load current varies by changing the load resistance in steps from 500 Ω at instant 0 sec up to 60 Ω at instant 2.75 sec as shown in Fig.9. The terminal voltage is affected by these load changes as shown in Fig.10 where the voltage drops sharply as the load current increases.

Also, wind speed variation is depicted in Fig.11 while the load resistance is kept constant at 100 Ω . In the case of constant excitation capacitance, any changes in wind speed affect the phase terminal voltage as shown in Fig.12.

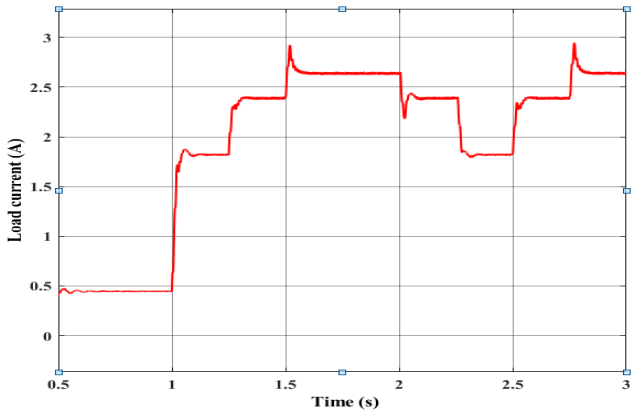


Fig.9. Load current variation at $V_{wind}=8m/s$ and $C=100 \mu F$.

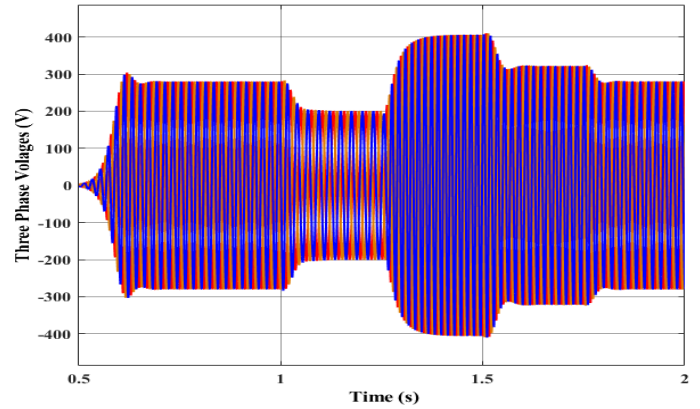


Fig.12. Three-phase voltages variation at $R_L=100\Omega$ and $C=100 \mu F$.

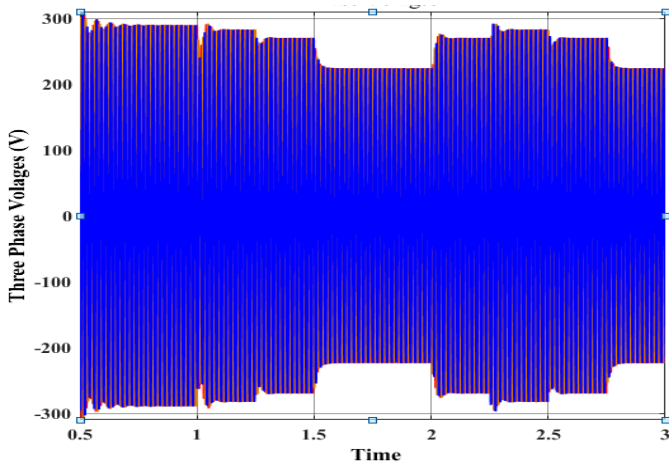


Fig.10. Three-phase voltages variation at $V_w=8m/s$ and $C=100 \mu F$.

4.1.2. *Balanced Operation by Regulating the Excitation Capacitance Using FC-SVC*

The previous case study shows how variations in wind speed and load have a significant impact on the SESRG output voltage under fixed excitation capacitance. As a result, the excitation capacitance must be carefully adapted to maintain a constant terminal voltage regardless of changes in load or wind speed.

In this case, the terminal voltage is controlled within a constant level by the excitation capacitance adaptation using FC-SVC based on ANN. The implementation of ANN is used for the online prediction of the optimum excitation capacitance and then calculates the corresponding TCR firing angle to obtain the required excitation capacitance at the generator terminals.

Figure 13 is shown the load variations by changing the load resistance in steps from 500Ω up to 60Ω at an instant of 4sec. Figure 14 depicts the controlled terminal phase voltage, which demonstrates that the terminal voltage is regulated to be constant regardless of load changes. The ANN online predicts the required excitation capacitance and then calculates the TCR firing angle for each load condition, as illustrated in Fig.15-16. Consequently, the terminal voltage rms value is almost constant regardless of the changes in load current, as illustrated in Fig.17.

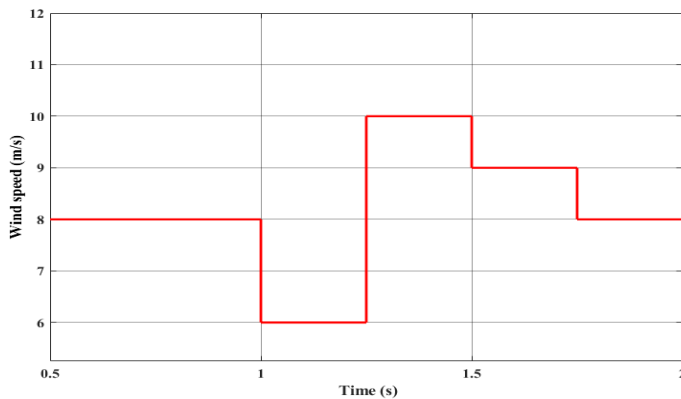


Fig.11. Wind speed variations.

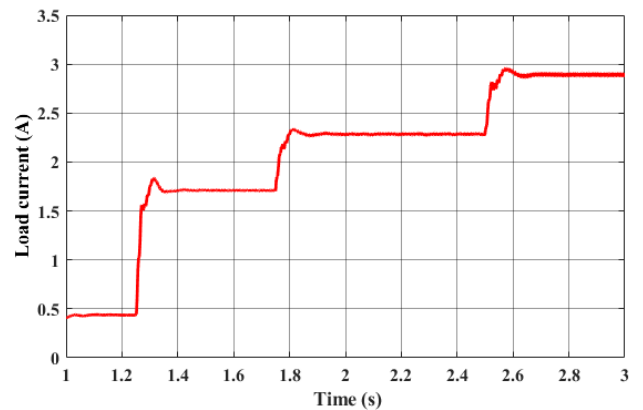


Fig.13. Load Current variation.

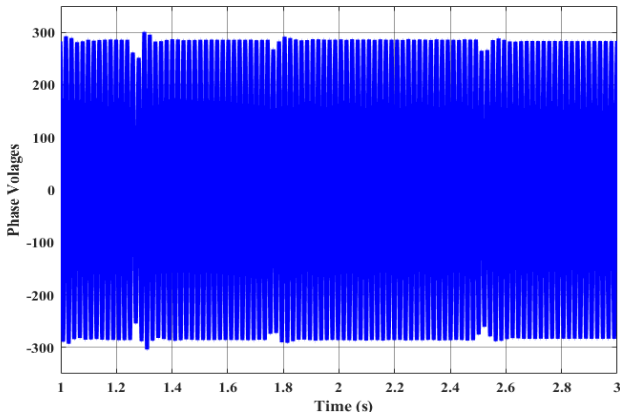


Fig.14. The phase voltage at terminal (a) at load changes.

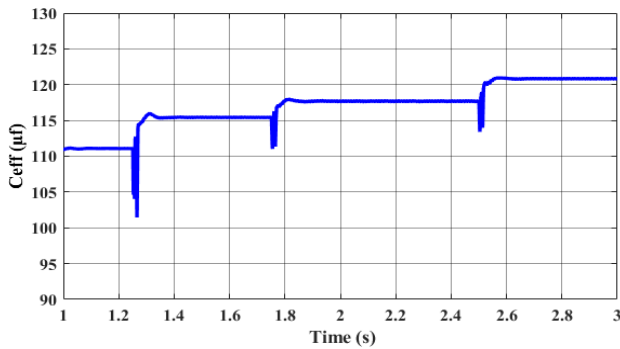


Fig.15. Effected Excitation Capacitance by SVC based on ANN prediction.

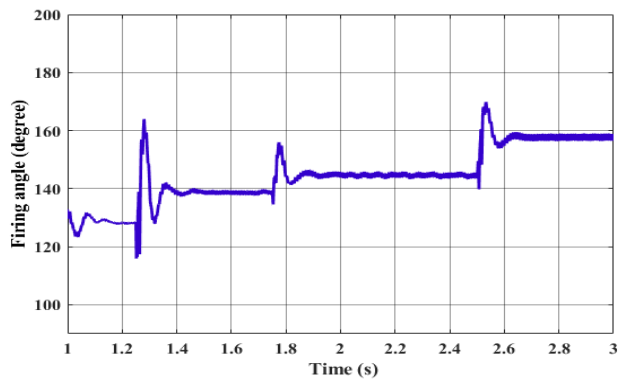


Fig.16. TCR Firing Angle variations at load changes.

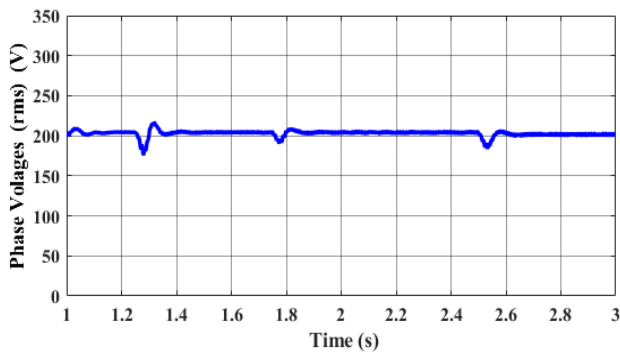


Fig.17. The R.M.S of terminal phase voltage against load current.

4.2. Case Study II

4.2.1. Unbalanced Operation

This case presents the results of SERG under unbalanced operation. The unbalanced conditions may take place by an unsymmetrical load. In case the unbalanced takes place in voltages and currents; then the positive and negative sequence components are produced. The positive and negative sequence components for voltages and currents are computed by using symmetrical components. In addition, the Voltage Unbalance Factor VUF is defined by employing the IEC definition.

$$VUF = \frac{V_s^-}{V_s^+} * 100 \tag{20}$$

For this case, the SVC based on ANN is used to mitigate the unbalance condition by controlling the excitation capacitance individually for each phase (C_a , C_b and C_c).

The unbalance condition is achieved by connecting the generator terminals to an unsymmetrical load. The resistive load connected to two phases (a) and (c) is the same, but the resistive load connected to phase (b) is varied from 1p.u to 1.5 p.u and increases until the open phase condition. Figure 18 shows the variation of positive and negative sequence components of voltages against the unbalance voltage factor UVF. The negative sequence voltage varies without SVC from 0 to 5.79% and 44.57% at open phase conditions, while it varies with SVC from 0% to 2.475% and 12.54% at open phase. In addition to the positive sequence, the voltage varied from 100% to 100.44% at the open phase and varied using SVC from 100% to 105% at open phase conditions. Figure 19 shows the effect of negative-sequence voltage on the negative-sequence current produced by SER. The resulting negative sequence current varies with the degree of unbalanced voltage factor almost linearly varied without SVC from 0 % to 42.63% and varied using SVC from 0% to 25.92%.

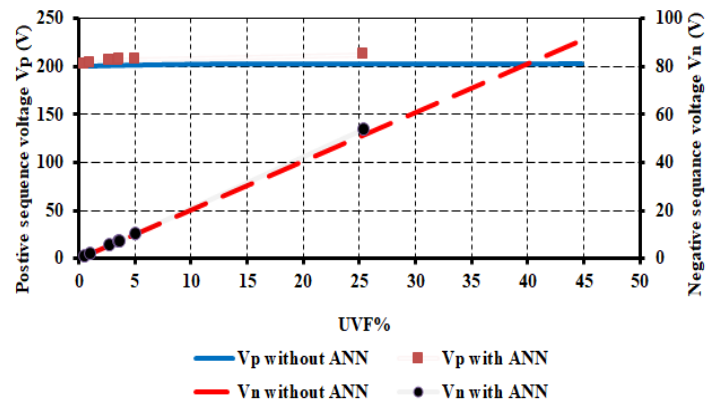


Fig.18. Variation of positive and negative sequence components of phase voltage against UVF at unsymmetrical load.

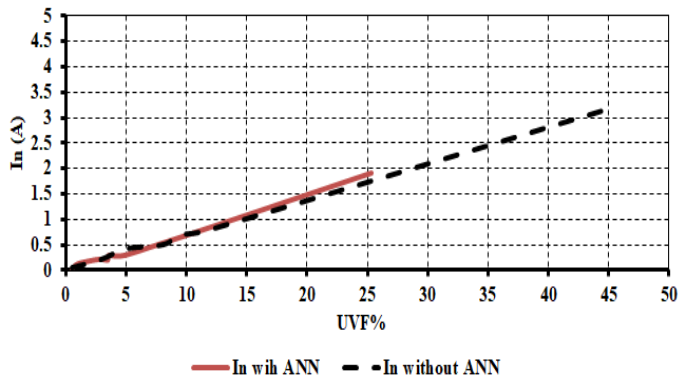


Fig.19. Variation of current negative sequence component against UVF at unsymmetrical load.

Figure 20 depicts the three-phase terminal voltage under balanced and unbalanced load conditions. The unbalanced condition is taking place by connecting load resistance at phase (b) = 1.2 and 1.4 pu respectively at instants 0.8 s and at 1 s. Figure 21 depicts the unbalanced three-phase voltage mitigation by injecting a three-phase current via SVC, as shown in Fig. 22.

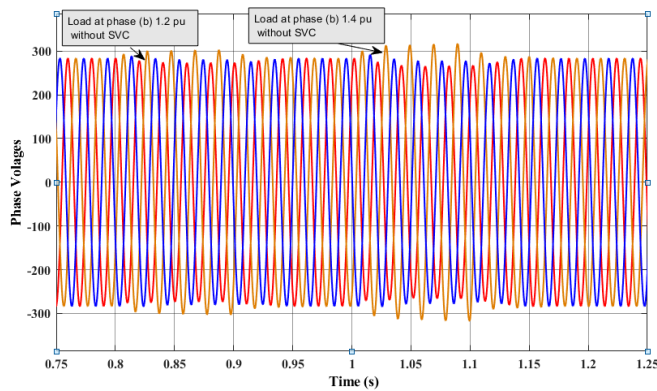


Fig.20. Unbalanced three-phase voltage without SVC

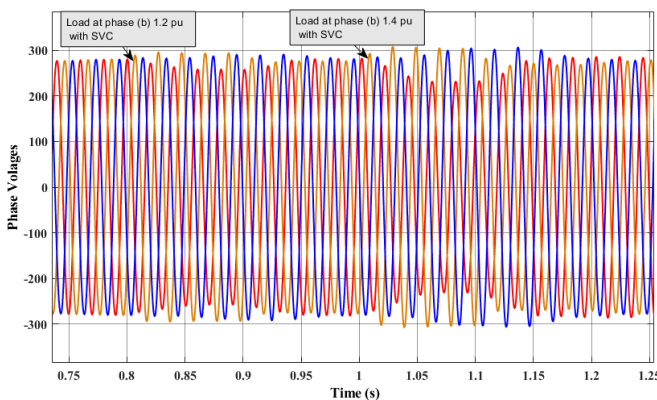


Fig.21. Unbalanced three-phase voltage with SVC.

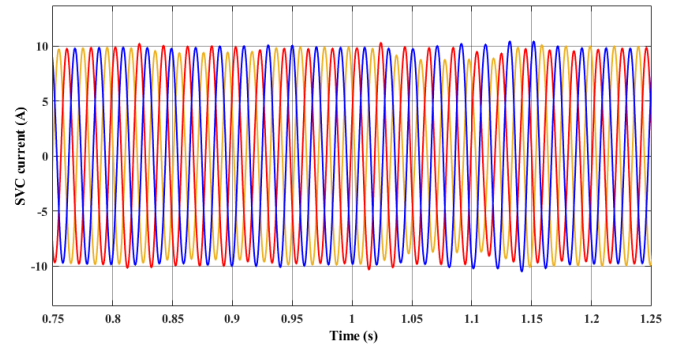


Fig.22. SVC current during unbalanced load condition.

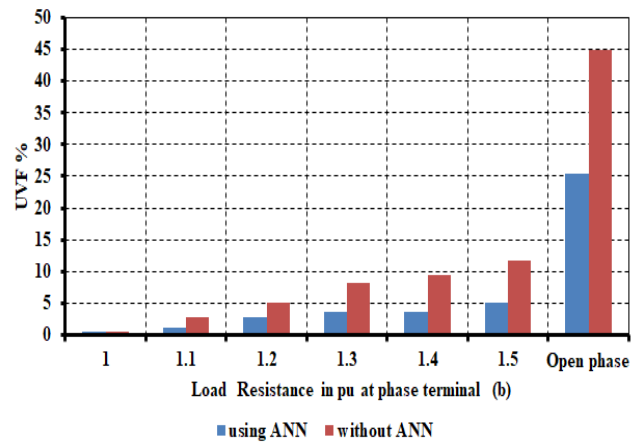


Fig.23. The UVF variation against unsymmetrical pu Resistive Load at phase (b).

Figure 23 shows the UVF variation against pu resistive load variation at the terminal (b). The UVF varied from 0% to 44.8% without VSC, while it varied from 0% to 25.2% in the SVC case.

5. Conclusions

The model of stand-alone SESRG driven by the wind turbine has been modeled using MATLAB/Simulink. The ANN based on SVC is designed and evaluated during load change and variable wind speed cases by predicting the excitation capacitance required to maintain the terminal voltage constant regardless of the changes in both load and wind speed. The simulation results are presented and discussed during the different case studies and compared to the fixed excitation capacitance case. The obtained results showed the performance of the voltage is kept constant using ANN based on SVC regardless of the changes in load cases and variable wind speed. Furthermore, the operation during the unbalanced load condition case study is studied in detail and the introduced positive and negative sequence components for voltages and currents are computed using the symmetrical components method. The excitation capacitance required for each phase is predicted individually by using ANN based on SVC. The individual prediction of the excitation capacitance using ANN minimized the VUF to 50% compared to using fixed excitation capacitance.

REFERENCES

- [1] K. Wei, Y. Yang, H. Zuo, and D. Zhong, "A review on ice detection technology and ice elimination technology for wind turbine", *Wind Energy*, DOI: 10.1002/we.2427, Vol. 23, No. 3, pp. 433–457, March 2020.
- [2] T. R. Ayodele, A. S. O. Ogunjuyigbe, and B. B. Adetokun, "Optimal capacitance selection for a wind-driven self-excited reluctance generator under varying wind speed and load conditions", *Applied Energy*, DOI: 10.1016/j.apenergy.2016.12.137, Vol. 190, pp. 339–353, March 2017.
- [3] M. M. Ali, S. M. Allam, and T. H. Abdel-Moneim, "Dynamic characteristics of an isolated self-excited synchronous reluctance generator driven by a wind turbine", *Turkish Journal of Electrical Engineering and Computer Sciences*, DOI: 10.3906/elk-1412-6, Vol. 24, No. 6, pp. 5238–5250, 2016.
- [4] A. E. Hoffer, R. H. Moncada, B. J. Pavez, J. A. Tapia and L. Laurila "A high-efficiency control strategy for synchronous reluctance generator including saturation", *International Conference on Electrical Machines (ICEM)*, pp. 39-45, 04-07 September 2016.
- [5] M. Deepu Vijay, B. Singh and G. Bhuvanewari, "Stand-alone and grid-connected operations of a SynRG based WECS with BESS", *IEEMA Engineer Infinite Conference (eTechNxT)*, pp. 1-6, 13-14 March 2018.
- [6] M. A. Esmaeel, "Steady State Analysis of A wind Energy Driven Self Excited Induction Generator (SEIG)", *8th International Conference on Smart Grid (icSmartGrid)*, pp. 101-108, 17-19 June 2020.
- [7] Calgan, E. Ilten, and M. Demirtas, "Thyristor controlled reactor-based voltage and frequency regulation of a three-phase self-excited induction generator feeding unbalanced load", *Int. Trans. Electr. Energy Syst.*, DOI: 10.1002/2050-7038.12387, Vol. 30, March 2020.
- [8] M. Ibrahim and P. Pillay, "The Loss of Self-Excitation Capability in Stand-Alone Synchronous Reluctance Generators", *IEEE Transactions on Industry Applications*, DOI: 10.1109/TIA.2018.2849407, Vol. 54, No. 6, pp. 6290-6298, December 2018.
- [9] A. S. O. Ogunjuyigbe, T. R. Ayodele, and B. B. Adetokun, "Steady state analysis of wind-driven self-excited reluctance generator for isolated applications", *Renewable Energy*, DOI:10.1016/j.renene.2017.07.110, Vol. 114, pp. 984–1004, December 2017.
- [10] S. S. Maroufian and P. Pillay, "Self-Excitation Criteria of the Synchronous Reluctance Generator in Stand-Alone Mode of Operation", *IEEE Transactions on industry application*, DOI:10.1109/TIA.2017.2764847, Vol. 54, No. 2, pp. 1245–1253, March 2018.
- [11] Y. Chaturvedi, "Effects of magnetization characteristics on the performance of self-excited induction generator under unbalanced operations", *International Journal of System Assurance Engineering and Management*, DOI: 10.1007/s13198-021-01281-x, Vol. 13, No. 1, pp. 375–384, February 2020.
- [12] E. L. Geraldi, T. C. C. Fernandes, A. B. Piardi, A. P. Grilo, and R. A. Ramos, "Parameter estimation of a synchronous generator model under unbalanced operating conditions", *Electric Power Systems Research*, DOI: 10.1016/j.epr.2020.106487, Vol. 187, October 2020.
- [13] E. Espina, J. Llanos, C. Burgos-Mellado, R. Cárdenas-Dobson, M. Martínez-Gómez and D. Sáez, "Distributed Control Strategies for Microgrids: An Overview", *IEEE Access*, Doi: 10.1109/ACCESS.2020.3032378, Vol. 8, pp. 193412–193448, October 2020.
- [14] V. P. Suppioni, A. P. Grilo, and J. C. Teixeira, "Improving network voltage unbalance levels by controlling DFIG wind turbine using a dynamic voltage restorer", *International Journal of Electrical Power and Energy Systems*, DOI: 10.1016/j.ijepes.2017.10.002, Vol. 96, pp. 185–193, March 2018.
- [15] J. Chhor, P. Tourou and C. Sourkounis, "On advanced control strategies for DFIG-based wind energy conversion systems during voltage unbalance", *IEEE 6th International Conference on Renewable Energy Research and Applications (ICRERA)*, pp. 331-338, 05-08 November 2017.
- [16] J. S. Sedky, H. M. Yassin, H. H. Hanafy, and F. Ismail, "Voltage and frequency control of stand-alone wind-driven self-excited reluctance generator using switching capacitors", *J. Electr. Syst. Inf. Technol.*, DOI: 10.1186/s43067-021-00030-1, Vol. 8, No. 1, December 2021.
- [17] Y. Wang and N. Bianchi, "Modeling and Investigation of Self-Excited Reluctance Generators for Wind Applications", in *IEEE Transactions on Industry Applications*, DOI: 10.1109/TIA.2019.2935931 Vol. 55, No. 6, pp. 5809-5817, Nov.-December 2019.
- [18] M. Rida, E. M. Rashad, Adel A. El-Samahy, M. I. El-Korfolly, and E. Youssef, "Performance Analysis of a Stand-Alone Synchronous Reluctance Generator under Unbalanced Conditions", *International Journal of Power Electronics and Drive System (IJPEDS)*, DOI: 10.11591/ijped.v14.i1.ppab-cd, Vol. 14, No. 1, March 2023.
- [19] B. T. Zine-Eddine, N. Ali, M. Said, and I. Rachid, "A New Control Method of Three-Phase Self Excited Induction Generator Feeding Single-Phase Load by using Static Var Compensator", *Int. Conf. Wind Energy Appl. Alger. ICWEAA*, pp. 1–5, 06-07 November 2018.
- [20] H. Su, C. Yang, H. Mdeihly, A. Rizzo, G. Ferrigno, and E. De Momi, "Neural network enhanced robot tool identification and calibration for bilateral teleoperation", *IEEE Access*, DOI: 10.1109/ACCESS.2019.2936334, Vol. 7, pp. 122041–122051, August 2019.
- [21] S. Della Krachai, A. Boudghene Stambouli, M. Della Krachai, and M. Bekhti, "Experimental investigation of artificial intelligence applied in MPPT techniques", *Int. J. Power Electron. Drive Syst.*, DOI:

- 10.11591/ijpeds.v10.i4.2138-2147, Vol. 10, No. 4, pp. 2138–2147, December 2019.
- [22] H. K. Khleaf, A. K. Nahar, and A. S. Jabbar, “Intelligent control of DC-DC converter based on PID-neural network”, *Int. J. Power Electron. Drive Syst.*, DOI: 10.11591/ijpeds.v10.i4.2254-2262, Vol. 10, No. 4, pp. 2254–2262, December 2019.
- [23] N. F. Fadzail, S. Mat Zali, M. A. Khairudin, and N. H. Hanafi, “Stator winding fault detection of induction generator based wind turbine using ANN”, *Indones. J. Electr. Eng. Comput. Sci.*, DOI: 10.11591/ijeecs.v19.i1.pp126-133, Vol. 19, No. 1, pp. 126–133, July 2020.
- [24] G. Bal, O. Kaplan and S. S. Yalcin, "Artificial Neural Network Based Automatic Voltage Regulator for a Stand-Alone Synchronous Generator", 8th International Conference on Renewable Energy Research and Applications (ICRERA), pp. 1032-1037, 03-06 November 2019.
- [25] A. Almadhor, "Performance prediction of distributed PV generation systems using Artificial Neural Networks (ANN) and Mesh Networks", International Conference on Smart Grid (icSmartGrid), pp. 88-91, 04-06 December 2018.
- [26] B. B. Adetokun, A. I. Adekitan, T. E. Somefun, A. Aligbe, and A. S. O. Ogunjuyigbe, “Artificial Neural Network-Based Capacitance Prediction Model for Optimal Voltage Control of Stand-alone Wind-Driven Self-Excited Reluctance Generator”, *IEEE PES/IAS PowerAfrica*, pp. 485–490, 28-29 June 2018.
- [27] A. Mohanty, M. Viswavandya, and S. Mohanty, “Prevention of Transient Instability and Reactive Power Mismatch in a Stand-alone Wind-diesel-tidal Hybrid System by an ANN Based SVC”, *Aquat Procedia*, Vol. 4, pp. 1529–1536, 2015.
- [28] A. Rashad, S. Kamel, F. Jurado, M. Abdel-Nasser, and K. Mahmoud, “ANN-Based STATCOM Tuning for Performance Enhancement of Combined Wind Farms”, *Electric Power Components and Systems*, DOI: 10.1080/15325008.2019.1570052, Vol. 47, No. 1–2, pp. 10–26, Jan. 2019.
- [29] E. Rezaei, M. Ebrahimi, and A. Tabesh, “Control of DFIG Wind Power Generators in Unbalanced Microgrids Based on Instantaneous Power Theory”, *IEEE Transactions on Smart Grid*, DOI: 10.1109/TSG.2016.2521644, Vol. 8, No. 5, pp. 2278–2286, Sep. 2017.